

# Ceria in Catalysis: From Automotive Applications to the Water–Gas Shift Reaction

Raymond J. Gorte

Dept. of Chemical and Biomolecular Engineering, University of Pennsylvania, Philadelphia, PA 19104

DOI 10.1002/aic.12234

Published online March 3, 2010 in Wiley InterScience (www.interscience.wiley.com).

*Ceria is a crucial component of automotive catalysts, where its ability to be reduced and re-oxidized provides oxygen storage capacity. Because of these redox properties, ceria can greatly enhance catalytic activities for a number of important reactions when it is used as a support for transition metals. For reactions that use steam as an oxidant (e.g., the water–gas-shift reaction and steam reforming of hydrocarbons), rates for ceria-supported metals can be several orders of magnitude higher than that for ceria or the transition metal alone. Because the redox properties of ceria are strongly dependent on treatment history and the presence of additives, there are significant opportunities for modifying catalysts based on ceria to further improve their performance. This article will review some of the contributions from my laboratory on understanding and using ceria in these applications. © 2010 American Institute of Chemical Engineers AIChE J, 56: 1126–1135, 2010*

**Keywords:** ceria, thermodynamic properties, water–gas-shift reaction, steam reforming reaction, sulfur poisoning, supported-metal catalysts

## Introduction

Most metal catalysts exist in the form of small particles on high-surface-area supports, which are usually a metal oxide, such as silica, alumina, or titania, at least for gas-phase reactions. The support allows efficient use of the metal because reactions typically occur only on the surface of the metal. The particle size of the metal and the support composition can affect catalytic properties. Regarding particle size, it has been known for many years that the rates of some reactions depend on particle size (structure sensitive reactions) and some do not (structure insensitive).<sup>1</sup> Interest in catalyst-support interactions increased significantly with work from Exxon in the 1970s on strong metal-support interactions (SMSI), especially those associated with titania-supported catalysts.<sup>2</sup>

My own research in supported-metal catalysts grew out of an interest in determining how catalyst-support interactions<sup>3–6</sup> and metal particle size<sup>7–10</sup> influence adsorption properties and how these in turn affect reactions. One of the most intriguing

and commercially important examples for which “support” interactions play a crucial role is that of precious metals on cerium oxide (ceria). Ceria has been included in automotive, emissions-control catalysts for many years<sup>11–13</sup> and ceria-supported metals are finding new applications in water–gas-shift,<sup>14–17</sup> hydrocarbon-reforming,<sup>18,19</sup> and in hydrocarbon-oxidation<sup>20</sup> catalysis. In all of these applications, the ability of cerium to cycle between Ce<sup>+3</sup> and Ce<sup>+4</sup> is crucial; however, the mechanisms by which ceria promotes reactions are complex. Understanding these mechanisms is technologically important because the properties of ceria are strongly affected by its morphology, pretreatment conditions, and presence of dopants.

In this article, I will focus on some of the contributions that have come out of my laboratory on understanding and applying ceria to catalytic applications.

## Lessons from Automotive Catalysis

The widespread interest in the catalytic properties of ceria results from its application in automotive catalytic converters. The challenge in automotive catalysis is that oxidation of CO and hydrocarbons must be carried out simultaneously with reduction of NO<sub>x</sub>. The harsh conditions experienced in

R. J. Gorte's e-mail address is gorte@seas.upenn.edu.

the catalytic converter dictate that the catalysts be based on precious metals (e.g., Pt, Rh, and Pd), but precious metals are not selective for oxidizing CO and hydrocarbons using NO<sub>x</sub> in the presence of O<sub>2</sub>. Removal of all three major pollutants can only occur if the engine is operated at the stoichiometric, air:fuel ratio where the oxidation and reduction reactions are exactly balanced.<sup>12,13</sup> An oxygen sensor in the exhaust, together with computer management of the engine, allows for feedback control of the composition; but there are still the inevitable deviations from the set point composition in any control system. Ceria is added to catalytic formulations of three-way catalysts because of its ability to cycle between Ce<sup>+3</sup> and Ce<sup>+4</sup> (e.g., Ce<sub>2</sub>O<sub>3</sub> + 1/2 O<sub>2</sub> → 2CeO<sub>2</sub>) and, therefore, to buffer the exhaust composition through its oxygen-storage capacity (OSC).

At first examination, OSC appears to be a very simple concept. When excess O<sub>2</sub> is present in the exhaust stream, it is removed by adsorption onto reduced ceria so that CO and hydrocarbons are oxidized by reducing NO<sub>x</sub>. When there are insufficient amounts of NO<sub>x</sub> and O<sub>2</sub> in the exhaust to oxidize the CO and hydrocarbons, ceria releases oxygen. This release does not involve formation of gas-phase O<sub>2</sub> but is rather caused by the reduction of ceria by CO, hydrocarbons, or H<sub>2</sub>. However, a closer examination reveals that the role of ceria in automotive exhaust catalysis is far more complex and interesting.<sup>21</sup> Unraveling these mechanisms has also demonstrated that ceria could find utility in other applications.

First, if ceria were a simple oxygen capacitor, it should be possible to determine the OSC of a catalyst by measuring the amount of oxygen that can be removed and added when the catalyst is exposed to alternating CO and O<sub>2</sub> pulses. This is contradicted by the fact that simple CO–O<sub>2</sub> titration methods do not properly characterize what is happening in the catalytic converter. For example, Hepburn et al. reported “that the CO/O<sub>2</sub> titration method was unable to differentiate between catalysts which displayed greatly different transient performances on a vehicle.”<sup>22</sup> In a more dramatic demonstration of the problem (discussed in more detail later in this article), it was found that ceria-based catalysts were able to reversibly release much more oxygen in alternating CO–O<sub>2</sub> pulses after they have been exposed to SO<sub>2</sub>,<sup>23</sup> even though the loss of OSC upon the introduction of SO<sub>2</sub> in vehicles is well documented.

Second, the details for how oxygen is transferred to and from ceria are not simple. It is well established that reduction of ceria requires contact with the precious metals. Although this suggests that some kind of “spillover” process must exist at the metal–ceria interface, the details of this process are not well understood. Furthermore, pure ceria is not stable and quickly loses its OSC properties when applied in a vehicle. In practical catalysts, ceria is in the form of a mixed oxide with zirconia.<sup>11</sup> It is sometimes reported that deactivation of ceria is due to the loss of surface area, but ceria–zirconia-mixed oxides work quite well even though they exhibit similar losses in surface area.

Finally, there are a number of related issues concerning the role of ceria in catalysis. For example, the oxygen-ion conductivity of ceria can be increased significantly by doping with other rare-earth cations<sup>24</sup> and it is reasonable to expect that ionic conductivity could affect OSC through

transfer of oxygen from the bulk. Doping of ceria may also affect oxygen binding in ceria.<sup>25</sup> In addition, ceria has been suggested for use in sulfur traps,<sup>26</sup> which is especially interesting given the strong sensitivity of automotive catalysts to sulfur poisoning.<sup>27,28</sup>

## Oxygen Transfer to Precious Metals

Our earliest work examined metal–ceria interfaces by vapor depositing catalytic metals onto polycrystalline ceria films in ultra-high vacuum, then measuring the adsorption properties of the metals using temperature-programmed desorption (TPD) of various adsorbates, such as CO,<sup>29</sup> H<sub>2</sub>, and NO.<sup>30</sup> The primary advantage of studying flat, model catalysts is that TPD measures the intrinsic desorption and surface-reaction rates, without the complications of readsorption and diffusion that can increase the temperature to which adsorbates remain on the catalyst surface by several hundred degrees.<sup>31,32</sup>

Results for CO adsorption on Pd/ceria are shown in Figure 1 but the conclusions from measurements on Pt/ceria and Rh/ceria were similar.<sup>30</sup> The data in Figure 1a were obtained following room temperature adsorption of CO on a Pd film that was freshly deposited onto oxidized ceria. The Pd film was ~5 atomic layers thick and agglomerated into particles with an average diameter of about 9 nm after heating to 700 K. There was no adsorption of CO in the absence of Pd; and the shapes of the CO desorption features in Figure 1a are identical to that obtained from Pd particles on α-Al<sub>2</sub>O<sub>3</sub>(0001),<sup>33</sup> implying that Pd is not chemically altered by the presence of ceria. More significantly, ~20% of the adsorbed CO reacted to CO<sub>2</sub> before desorption and the source of the oxygen to form the CO<sub>2</sub> could only be the underlying ceria. Repeated cycles of CO adsorption and desorption were similar to that shown in Figure 1a, except that the amount of CO<sub>2</sub> decreased monotonically, until very little CO<sub>2</sub> was observed leaving the sample in which the ceria had been reduced, as shown in the TPD curves of Figure 1b. It is also noteworthy that annealing the sample to higher temperatures so as to allow oxygen from the ceria bulk to diffuse to the surface would restore the CO<sub>2</sub> desorption feature.

In principle, the results in Figure 1 could be explained by reaction of CO on the Pd with oxygen from the ceria at the periphery of the Pd particles. However, given that the fraction of CO which reacts is higher than the fraction of periphery sites and that the CO<sub>2</sub> forms at a temperature similar to that which would be expected from coadsorbed CO and oxygen, it seems more likely that Pd is being oxidized by ceria. Additional evidence for the oxidation of Pd by ceria comes from an X-ray Photoelectron Spectroscopy study by Smirnov and Graham.<sup>34</sup> They demonstrated that metallic Pd deposited onto a ceria–zirconia film became completely oxidized when heated to 673 K in high vacuum. They reported that this result was particularly surprising given that it is difficult to oxidize the bulk of Pd by exposure to gas-phase O<sub>2</sub> in a high-vacuum chamber.

Oxygen transfer from ceria to a precious metal has important implications for catalysis, as demonstrated by reaction rates for CO oxidation on ceria-supported metals.<sup>35–38</sup> In excess CO, the kinetics for this reaction over bulk Pt, Pd,

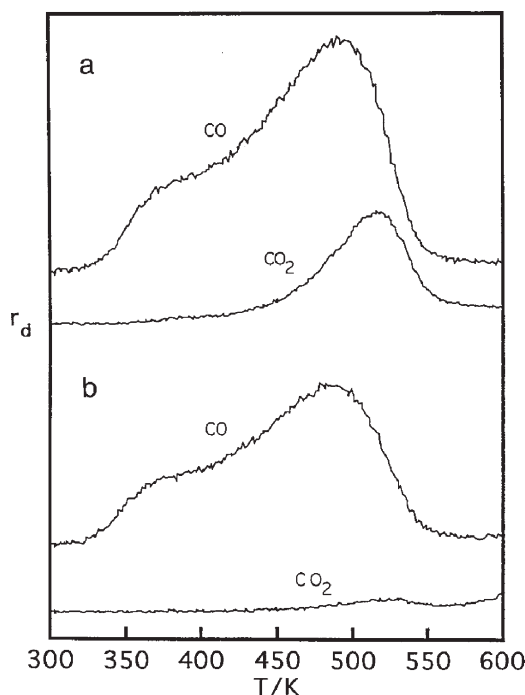
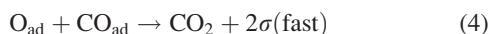
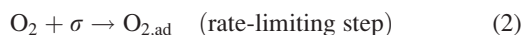
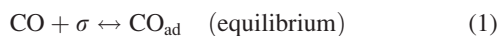


**Figure 1. Saturation TPD curves following CO adsorption at room temperature on a film of  $5 \times 10^{15}$  Pd/cm<sup>2</sup>.**

(a) As deposited on ceria ("fresh") and (b) after mild reduction in CO ("reduced"). (Reproduced from Ref 30).

and Rh are very well understood and are well described by Reactions 1 through 4, where  $\sigma$  represents an empty site on the metal. Because the metal surfaces are essentially saturated in CO when excess CO is present, the rate-limiting step for the reaction is the adsorption of O<sub>2</sub>.



The activation energy for Reaction 2 is nearly 0, so that this mechanism predicts the overall reaction should be first order in O<sub>2</sub> and inverse-first-order in CO, with an activation energy equal to the heat of adsorption of CO.<sup>10</sup> With ceria-supported metals, there is an additional pathway for forming O<sub>ad</sub> by transfer of oxygen from ceria to the metal, shown in Reaction 5.

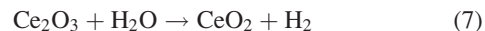


Because ceria does not adsorb CO, the reoxidation of Ce<sub>2</sub>O<sub>3</sub>, Reaction 6, is not affected by the coverage of CO on the metal. When Reaction 5 is rate limiting, the rate is predicted to be zeroth-order in CO, with an activation energy

equal to that of Reaction 5. Although the activation energy of Reaction 5 is not known, it should be different from the heat of adsorption.

A change of mechanism is indeed observed, as demonstrated by the rate data in Figure 2 for CO oxidation over model Rh/alumina and Rh/ceria catalysts. Figure 2 shows differential reaction rates as a function of CO partial pressure, for a fixed O<sub>2</sub> pressure of 0.3 torr. Over Rh/alumina, the reaction is clearly inverse, first order in CO.<sup>35</sup> Over Rh/ceria, the rates are the same as those over Rh/alumina at the lower CO pressures but become independent of CO pressure at the higher pressures. This observation is easily explained by assuming that Reactions 2 and 5 are independent and that the overall rate is a simple sum of the rates for the two mechanisms. Examination of the temperature dependences showed that the activation energy for the inverse, first-order reaction was ~25 kcal/mol, similar to the heat of adsorption for CO on Rh, whereas the activation energy for the zeroth-order process was much lower, ~12 kcal/mol. Similar results were obtained on Pt/ceria and Pd/ceria catalysts.<sup>37</sup>

Reaction 5 has important implications for a number of reactions in addition to CO oxidation. Unlike precious metals which are ineffective for dissociation of water and CO<sub>2</sub>, reduced ceria is readily oxidized by H<sub>2</sub>O<sup>39</sup> and CO<sub>2</sub>.<sup>40</sup> Using steam as the oxidant, Reaction 6 is replaced by Reaction 7.



This, together with the ability of ceria to transfer oxygen to supported metals, leads to interesting possibilities for using steam and CO<sub>2</sub> as oxidants. For example, replacing O<sub>2</sub> in Reaction 6 with H<sub>2</sub>O results in the water-gas shift reaction, which is very important for the production of H<sub>2</sub>. Because CH<sub>4</sub> reacts readily with adsorbed oxygen on Pt, Pd, and Rh, this set of mechanistic steps also predicts that the ceria-supported metals should be good catalysts for oxidation of methane by steam (i.e., methane-steam reforming).<sup>41,42</sup> Indeed, a comparison methane steam-reforming rates over Pd/ceria, Pd/silica, and pure ceria in Figure 3 shows that the

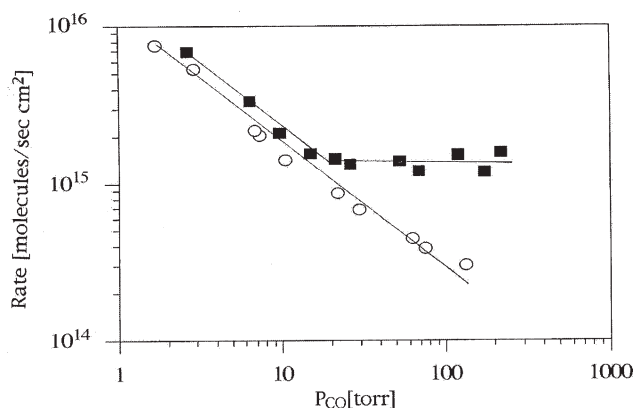


**Figure 2. CO oxidation rates on model Rh/ceria catalysts (■) and on model Rh/alumina catalysts (○) for 0.3 torr of O<sub>2</sub> at 573 K.**

(Reproduced from Ref 36).

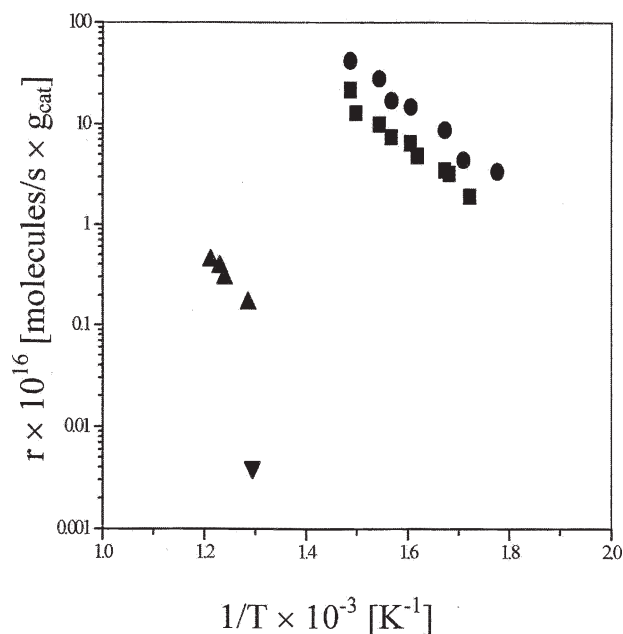


**Figure 3. Arrhenius plot for steam reforming of methane over porous catalysts prepared by impregnation of  $\text{Pd}(\text{NO}_3)_2$ .**

Results are shown for 1% Pd on ceria (■), 10% Pd on ceria (●), 10% Pd on silica (▼), and pure ceria (▲). Data were taken with 15 torr  $\text{H}_2\text{O}$  and 5 torr  $\text{CH}_4$ . (Reproduced from Ref 18).

Pd/ceria is at least 100 times as active as Pd/silica and  $10^4$  times as active as pure ceria.<sup>18</sup>

The fact that ceria-supported, precious metals exhibit high reaction rates for the water–gas-shift and hydrocarbon-steam-reforming reactions is significant. First, better water–gas-shift and steam-reforming catalysts are still needed. The most active, commercial, water–gas-shift catalysts (e.g., Cu/ZnO/alumina) are pyrophoric, must be treated very carefully to maintain their activity, and cannot be applied to small-scale fuel processors, such as might be needed in fuel-cell applications.<sup>14</sup> Even with regards to the automotive catalytic converter, the observation that ceria-supported metals help generate  $\text{H}_2$  is likely very significant, since the presence of  $\text{H}_2$  in the exhaust has been reported to lead to improved NO conversion.<sup>43</sup> Furthermore, given that the oxygen sensors used in monitoring  $P(\text{O}_2)$  are electrochemical devices based on the same principles as solid-oxide fuel cells (SOFC) and that most SOFC are much more sensitive to  $\text{H}_2$  than they are to CO or hydrocarbons,<sup>44,45</sup> reactions that generate  $\text{H}_2$  in the catalytic converter may well influence the control system.

### Deactivation of Ceria

As mentioned earlier, three-way catalysts use mixed oxides of ceria and zirconia for oxygen storage because pure ceria is not stable and quickly loses its OSC properties. Some of the lost activity is associated with a loss in surface area but deactivation cannot be solely due to this, since both ceria and ceria–zirconia-mixed oxides undergo similar losses in surface area and ceria–zirconia solutions are stable. To distinguish intrinsic changes in the ceria from lost surface

area, we again examined a series of model catalysts prepared by vapor deposition of the metal onto polycrystalline ceria films. Preparing catalysts in this way allows the metal particle size and ceria-metal contact area to be kept constant while changing the properties of the ceria support. Deactivation of the ceria component was simulated by calcining the ceria films in air to increasingly higher temperatures before the addition of the metal.

The model studies showed that the ability of ceria to transfer oxygen to a supported metal is lost when the ceria is calcined to high temperatures.<sup>46</sup> First, TPD studies showed that Rh particles deposited onto ceria films that were formed by calcination of  $\text{Ce}(\text{NO}_3)_3$  at 970 K were reactive for adsorbed CO. Following room-temperature adsorption, significant amounts of  $\text{CO}_2$  left the surface, similar to what is shown in the TPD of Figure 1a for Pd particles. When the Rh particles were deposited onto a  $\text{CeO}_2(100)$  crystal or a ceria film that had been heated in air to 1720 K, all of the CO desorbed intact at the same temperatures observed for CO desorption from Rh particles on  $\alpha\text{-Al}_2\text{O}_3(0001)$ .<sup>8</sup> The failure to form  $\text{CO}_2$  on the high-temperature forms of ceria was not due to the ceria substrate having been reduced by heating. This was demonstrated spectroscopically and by the fact that strong interactions between Rh and reduced ceria would have caused significant changes in the TPD desorption features had the ceria been reduced.<sup>47</sup>

The changes in the ability of ceria to transfer oxygen were also observed in steady-state reactions. In Figure 4, CO-oxidation rates are shown as a function of  $P(\text{CO})$ , at constant  $P(\text{O}_2)$  and temperature, for a series of model Pd/ceria catalysts.<sup>48</sup> As in the TPD studies, the ceria substrate

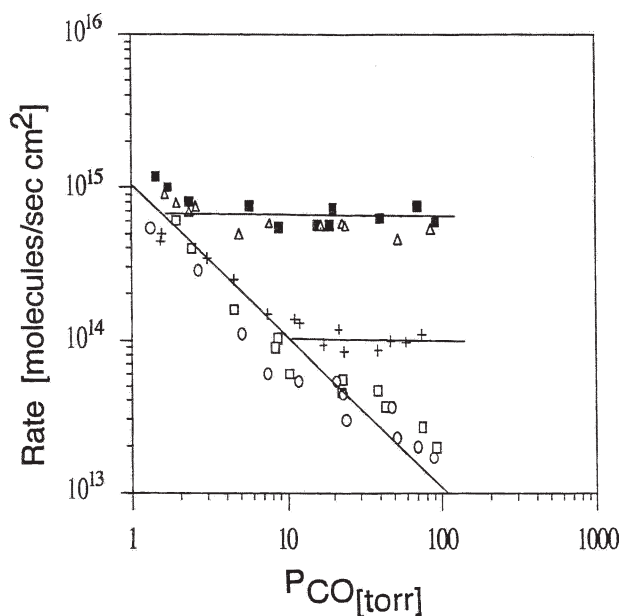


**Figure 4. Steady-state CO oxidation rates as a function of the CO partial pressure at 515 K for  $2 \times 10^{15}$  Pd/cm<sup>2</sup> film on the ceria film annealed at 570 K (■), 1070 K (Δ), 1170 K (+), 1270 K (○), and 1670 K (□).**

The  $\text{O}_2$  pressure was fixed at 0.3 torr. (Reproduced from Ref 48).



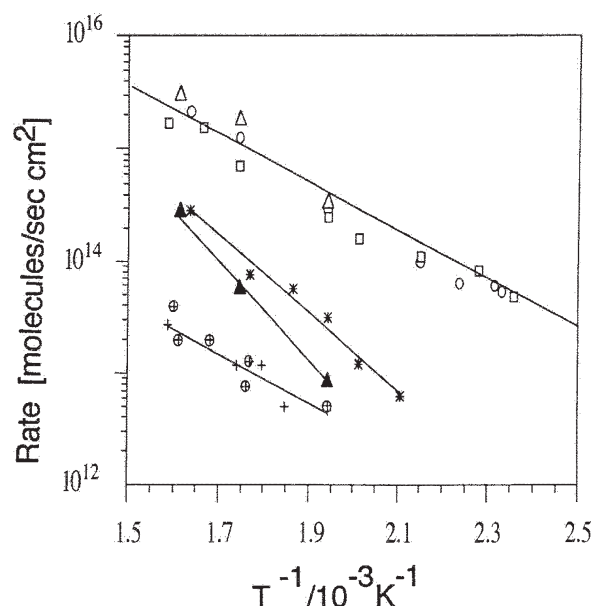


**Figure 5.** An Arrhenius plot for the water-gas-shift rates on alumina (+), ceria (\*),  $5 \times 10^{15}$  Rh/cm<sup>2</sup> on alumina ( $\otimes$ ),  $2 \times 10^{15}$  Pd/cm<sup>2</sup> on ceria (calined at 570 K) ( $\Delta$ ),  $2 \times 10^{15}$  Pd/cm<sup>2</sup> on ceria (1670 K) ( $\blacktriangle$ ),  $5 \times 10^{15}$  Rh/cm<sup>2</sup> on ceria (570 K) ( $\circ$ ), and  $5 \times 10^{15}$  Pt/cm<sup>2</sup> on ceria (570 K) ( $\square$ ).

The CO and H<sub>2</sub>O partial pressures were 20 and 15 torr, respectively. (Reproduced from Ref 49).

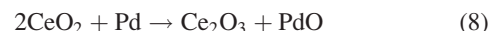
was formed by decomposing Ce(NO<sub>3</sub>)<sub>3</sub> and calcining in air to increasingly higher temperatures before vapor deposition of Pd particles. As there was a large excess of CO under all conditions, rates for Pd on a non-interacting support would exhibit an inverse first-order dependence on P(CO). This is exactly what is observed for the samples in which ceria was calcined above 1270 K. Samples from the ceria that was calcined at temperatures less than 1070 K exhibited the zeroth-order dependence discussed for the Rh/ceria catalyst in Figure 2, indicating that there was a second reaction pathway involving transfer of oxygen from ceria. The fact that all catalysts show similar rates in the inverse first-order region is a strong indication that the Pd dispersion was the same in all cases. It is interesting to note that the transition between showing the zeroth-order rate process or not occurred following ceria calcination over a very narrow range of temperatures, between 1070 and 1270 K. X-ray diffraction showed no change in structure or dramatic change in crystallite size in this temperature region. Finally, when experiments similar to those shown in Figure 4 were performed using films composed of ceria-zirconia-mixed oxides, a zeroth-order rate process was observed even for catalysts made from films heated to 1470 K, demonstrating the enhanced stability of ceria-zirconia mixtures.<sup>49</sup>

Figure 5 provides additional evidence for changes in the properties of ceria with calcination temperature for the water-gas-shift reaction.<sup>49</sup> The rates in this figure were normalized to the external surface areas of the films. The rates on alumina and Rh/alumina are so low they likely result

from reaction on the reactor walls, a problem that occurs due to the very low active area of the model catalysts. Although water-gas-shift rates on ceria are low, some activity was observed in these studies because the ceria films formed by deposition of Ce(NO<sub>3</sub>)<sub>3</sub> on alumina were porous, so that normalizing the rates to the external surface area over estimates what the specific rates on ceria really are. The significant point to be taken from this data is that catalysts formed by vapor deposition of Pt, Pd, or Rh onto ceria films that had been heated to only 570 K showed similar rates that were much higher than those on the ceria support or on the alumina-supported catalysts. Furthermore, when the ceria film was heated to 1670 K before the addition of Pd, the rates were much lower and exhibited a much higher activation energy. These results are again consistent with oxygen transfer from ceria to the metal assisting the water-gas-shift reaction and with changes in the reducibility of the ceria film upon high-temperature treatment.

### Thermodynamic Properties for Ceria

To understand the nature of ceria deactivation, it is important to determine what changes occur in ceria that cause the decreased catalytic activity. An important clue comes from considering Reaction 8, which is similar to the reaction that Smirnov and Graham had shown occurs rapidly at 673 K for Pd deposits on ceria-zirconia films.



On the basis of standard handbook data, this reaction is endothermic by 295 kJ/mol of oxygen that is transferred. Although the reduced form of ceria is unlikely to be Ce<sub>2</sub>O<sub>3</sub>, the enthalpy change per oxygen removed from the CeO<sub>2</sub> lattice has been reported to be essentially independent of the ceria oxygen stoichiometry,<sup>50</sup> so that the reaction enthalpy should be unaffected by the extent of ceria reduction. Strongly endothermic reactions obviously do occur; however, the activation energy for transfer of one mole of oxygen from CeO<sub>2</sub> to Pd must be at least as large as the enthalpy for that reaction. No simple model based on transition state theory can provide a rate-constant pre-exponential large enough to explain the low-temperature oxygen transfer reported by Smirnov and Graham or the apparent oxygen transfer that we observed in TPD from ceria films in Figure 1.

The calculated enthalpy change for Reaction 8 is dominated by the oxidation enthalpy for Ce<sub>2</sub>O<sub>3</sub> ( $\Delta H^\circ = -380$  kJ/mol of O). Because there are reports that the reducibility of ceria depends on crystallite size and shape,<sup>51</sup> we set out to quantify the equilibrium properties of different forms of ceria. The most reliable means for obtaining oxidation enthalpies involves measuring equilibrium data for Reaction 9:



Because the activities of the solid phases are unity, the equilibrium constant for Reaction 9 is equal to  $P(\text{O}_2)^{-1/2}$  and reaction enthalpies can be determined from the

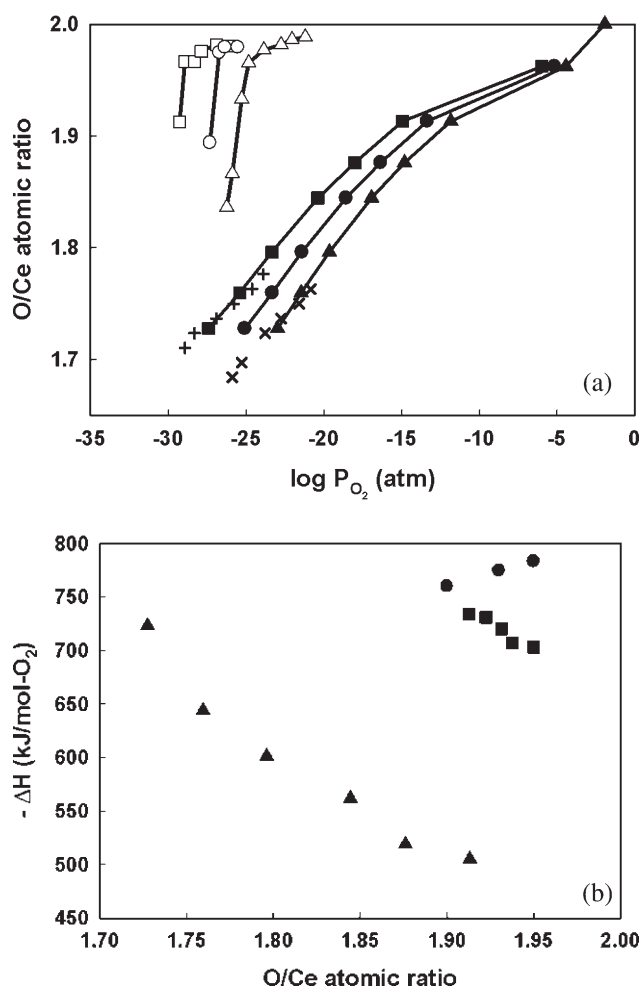


**Figure 6. (a) Oxidation isotherms for pure ceria (open symbols) and 30 wt % ceria/La-doped alumina (LA) (filled symbols) at selected temperatures (■873 K, ●923 K, ▲973 K); (b)  $-\Delta H$  of oxidation at 973 K for (▲) 30 wt % ceria/LA, (■)  $\text{Ce}_{0.8}\text{Sm}_{0.2}\text{O}_{1.9}$ , and (●) pure ceria as a function of extent of reduction.**

The (+) and (x) symbols show the isotherms for 30 wt % ceria/LA determined by flow titration at 873 and 973 K, respectively, and were taken to check the results obtained from coulometric titration. (Reproduced from Ref 51).

temperature dependence of the equilibrium constant. As the equilibrium  $P(\text{O}_2)$  at reasonable temperatures are very low and should be viewed as  $\text{O}_2$  fugacities rather than partial pressures, the  $P(\text{O}_2)$  must be established by equilibrium with  $\text{H}_2\text{-H}_2\text{O}$  or  $\text{CO-CO}_2$  mixtures.<sup>52</sup>

In our laboratory, we used two experimental methods for measuring equilibrium. In the first, we simply flowed  $\text{H}_2\text{-H}_2\text{O}$  mixtures over samples at the temperature of interest, then measured the oxidation state of the sample by titrating the amount of  $\text{O}_2$  required to oxidize it.<sup>53</sup> Although this method is simple and works well, the range of  $P(\text{O}_2)$  that can be measured is limited by the  $\text{H}_2\text{:H}_2\text{O}$  ratios that can be achieved reliably. The second technique, coulometric titration, measures the oxygen chemical potential electrochemically, using the same principles as that used in the oxygen sensor in automo-

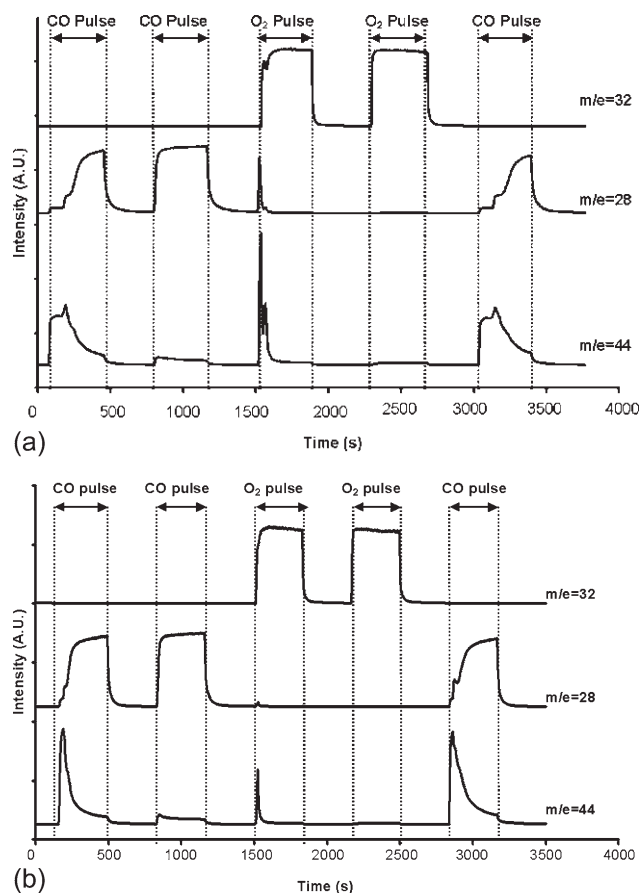
biles.<sup>52</sup> Because the sensor is based on an oxygen-ion membrane, oxygen is also added or removed from the sample electrochemically.

Figure 6 shows isotherm data and differential oxidation enthalpies for bulk ceria and for 30 wt % ceria on La-modified alumina.<sup>51</sup> When supported on La-modified alumina, the ceria was found to exhibit stable redox properties during the course of our experiments. The properties of bulk ceria were found to change after redox cycling and the data shown in this figure were obtained on a sample that had undergone multiple redox cycles at high temperatures. The bulk-ceria data in Figure 6 are essentially identical to what has been reported in the literature.<sup>50</sup> Figure 6a shows that significantly higher  $P(\text{O}_2)$  are required to keep the supported ceria in a highly oxidized state compared to that necessary for the bulk ceria. The oxidation enthalpies, shown per mole  $\text{O}_2$  in Figure 6b, were also quite different for the two samples. The oxidation enthalpies were determined to be between  $-750$  and  $-800$  kJ/mol  $\text{O}_2$  for bulk ceria, in reasonable agreement with the handbook value of  $-760$  kJ/mol  $\text{O}_2$ . For the supported catalyst, the oxidation enthalpy was a strong function of stoichiometry, starting at  $-500$  kJ/mol  $\text{O}_2$  for low extents of reduction and approaching the value for bulk ceria at higher extents. Interestingly, oxidation enthalpies measured on ceria-zirconia solid solutions were also found to be  $\sim -500$  kJ/mol  $\text{O}_2$ , but were independent of Ce:Zr ratio and oxygen stoichiometry in that case.<sup>52-54</sup>

The obvious question is what causes the thermodynamic properties of ceria to change in each of these systems. For ceria-zirconia solid solutions, there is evidence for plateaus in the isotherm at stoichiometries corresponding to the formation of  $\text{Zr}_2\text{Ce}_2\text{O}_7$ <sup>52</sup>; therefore, it seems likely that local compound formation within the bulk of the oxide drives the thermodynamic properties of these mixed oxides.<sup>52</sup> For pure ceria, none of our available techniques provided an obvious answer. The results could not be explained by differences between surface and bulk or by crystallite size, as the section on Deactivation of Ceria also showed.

Although our proposal remains speculative, we suggest that low-temperature forms of ceria have hydroxyls and defects that make them poorly ordered on the local scale. Evidence that reducible forms of ceria have a different average local structure, on the atomic scale, has indeed been observed in neutron scattering.<sup>55</sup> The local, cubic structure is critical for stabilizing  $\text{Ce}^{+4}$ ,<sup>56</sup> a fact that is demonstrated by the observation that  $\text{Ce}^{+3}$  is the more stable species in many other environments. For example, even though  $\text{Ce}_2\text{O}_3$  is readily oxidized by water,  $\text{Ce}^{+4}$  is a strong oxidizing agent in aqueous solutions. In  $\text{CeVO}_4$ , the oxidation states of the two metal cations are  $\text{Ce}^{+3}$  and  $\text{V}^{+5}$ ,<sup>56,57</sup> even though  $\text{V}_2\text{O}_5$  reduces very easily compared to  $\text{CeO}_2$ .<sup>58</sup> Therefore, we suggest that high-temperature treatment removes internal hydroxyls and other defects, locking all of the ceria into the fluorite structure and increasing the stability of  $\text{Ce}^{+4}$  relative to  $\text{Ce}^{+3}$ .

Independent of the reasons for the enhanced reducibility of low-temperature ceria, an oxidation enthalpy of  $-500$  kJ/mol  $\text{O}_2$  is able to explain why Reaction 7 can occur rapidly at moderate temperatures. The reaction is still expected to be endothermic but the barrier height could be as low as 165 kJ/mol of O, using bulk data for oxidation of Pd. As TPD studies suggest oxygen may adsorb somewhat more strongly on small Pd particles,<sup>59</sup> the barrier could be even lower. In



**Figure 7. Pulse measurements on (a) fresh and (b)  $\text{SO}_2$ -poisoned Pd/ceria catalysts at 723 K.**

The data are for two pulses of CO ( $m/e = 28$ ), followed by two pulses of  $\text{O}_2$  ( $m/e = 32$ ) and another of CO. Formation of  $\text{CO}_2$  ( $m/e = 44$  and 28) is observed. (Reproduced from Ref 23).

any case, 165 kJ/mol is a reasonable barrier for a reaction that occurs rapidly at 500 K, assuming typical pre-exponential factors derived from Transition-State Theory.

### The Effect of Sulfur on OSC

Sulfur is a severe poison for automotive, three-way catalysts. Although  $\text{SO}_2$  in the exhaust can poison precious-metal sites in high-sulfur fuels, a more serious problem at modest sulfur levels is that  $\text{SO}_2$  reacts with  $\text{CeO}_2$  to form cerium sulfates.<sup>27</sup> There is some evidence from infrared spectroscopy that one can distinguish between surface and bulk sulfates, but TPD studies of ceria exposed to  $\text{SO}_2$  under oxidizing conditions suggest that surface and bulk sulfates exhibit similar chemistry. TPD studies showed decomposition to  $\text{SO}_2$  and  $\text{O}_2$  of both surface and bulk sulfates occurs between 873 and 1073 K.

To understand how sulfur affects OSC, we examined the response of a 1 wt % Pd/ceria catalyst to alternating pulses of CO and  $\text{O}_2$  at 723 K, before and after poisoning the catalyst by exposing it to 1%  $\text{SO}_2$  in  $\text{O}_2$  at 673 K for several hours.<sup>23</sup> The results for the unpoisoned catalyst in Figure 7a show that significant amounts (500  $\mu\text{mol/g}$ ) of  $\text{CO}_2$  ( $m/e =$

44) were formed when CO was pulsed over an oxidized catalyst. An additional amount of  $\text{CO}_2$  (300  $\mu\text{mol/g}$ ) formed when the catalyst was subsequently re-oxidized by an  $\text{O}_2$  pulse due to decomposition of carbonates that are stable only on reduced forms of ceria.<sup>40</sup> As reduction of PdO for a 1 wt % Pd catalyst would give only 100  $\mu\text{mol/g}$ , most of the oxygen removed from the sample by formation of  $\text{CO}_2$  must come from reduction of the ceria. The results obtained on the same catalyst after poisoning with  $\text{SO}_2$  are shown in Figure 7b. The amount of  $\text{CO}_2$  formed by pulsing CO over the oxidized, poisoned catalyst, 500  $\mu\text{mol/g}$ , was greater than that formed on the unpoisoned catalyst. Less  $\text{CO}_2$  formed during the  $\text{O}_2$  pulse, consistent with less carbonate formation on the sulfated ceria; but the total amounts of oxygen that could be removed at 723 K were similar for the poisoned and the unpoisoned catalyst. The source of the oxygen on the sulfated catalyst is almost certainly related to reduction of cerium sulfates to  $\text{Ce}_2\text{O}_2\text{S}$ , a fact confirmed by infrared spectroscopy and by X-ray Photoelectron Spectroscopy.<sup>60</sup>

A major difference between the fresh and sulfated catalysts is observed in the response of the catalyst to alternating pulses of CO and  $\text{H}_2\text{O}$  at 723 K, shown in Figure 8. For the fresh catalyst, Figure 8a, a pulse of CO onto a steam-

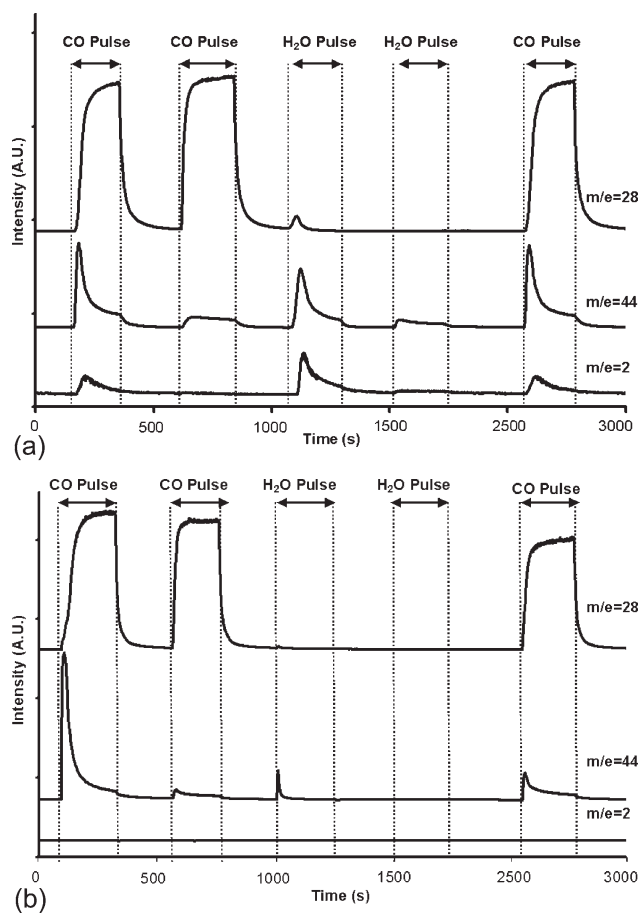


**Figure 8. Pulse measurements on (a) fresh and (b)  $\text{SO}_2$ -poisoned Pd/ceria catalysts at 723 K.**

The data are for two pulses of CO ( $m/e = 28$ ), followed by two pulses of  $\text{H}_2\text{O}$  and another of CO. (Reproduced from Ref 23).

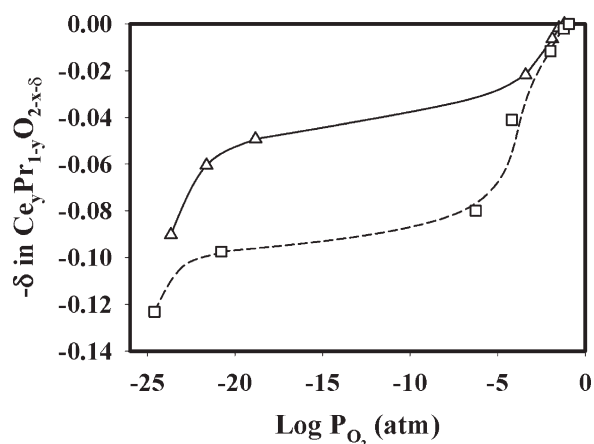


**Figure 9.**  $\delta$  in  $\text{Ce}_y\text{Pr}_{1-y}\text{O}_{2-x-\delta}$  as a function of  $P(\text{O}_2)$  at 973 K, for  $\text{Ce}_y\text{Pr}_{1-y}\text{O}_{2-x}$  calcined at 1323 K: (Δ)  $\text{Ce}_{0.8}\text{Pr}_{0.2}\text{O}_{2-x}$  and (□)  $\text{Ce}_{0.5}\text{Pr}_{0.5}\text{O}_{2-x}$ . (Reproduced from Ref 65).

oxidized sample resulted in the formation of 200  $\mu\text{mol/g}$  of  $\text{CO}_2$ , along with 100  $\mu\text{mol/g}$  of  $\text{H}_2$ . When the reduced sample was exposed to 2%  $\text{H}_2\text{O}$  in He, an additional 150  $\mu\text{mol/g}$  of  $\text{CO}_2$  and 250  $\mu\text{mol/g}$  of  $\text{H}_2$  were formed, demonstrating that the reduced ceria was being oxidized by steam. The result for a similar experiment on the  $\text{SO}_2$ -exposed catalyst is shown in Figure 8b, except that we started with an oxidized sample before beginning the pulse sequence. After reduction by the first CO pulse, the sample could not be reoxidized by steam. In confirmation of the CO– $\text{H}_2\text{O}$  pulse data, steady-state rates for the water–gas–shift reaction decreased by approximately two orders of magnitude after exposure to  $\text{SO}_2$ .<sup>23</sup>

The data in Figure 8, together with earlier statements about the importance of having  $\text{H}_2\text{O}$  present in measurements of OSC,<sup>21,22</sup> imply that the water–gas–shift plays an important role in OSC. Certainly, the partial pressure of  $\text{H}_2\text{O}$  in the exhaust is much greater than the partial pressure of  $\text{O}_2$ . The role of steam as an oxidant for ceria cannot be neglected.

### Effect of Thermodynamic Properties on WGS

Ceria-supported precious metals are active catalysts for the WGS reaction but higher rates would be desirable for some applications. On the basis of the mechanism for WGS in Reactions 1 through 5 and 7, the key steps are likely the transfer of oxygen to the metal sites, Reaction 5, and the oxidation of the ceria, Reaction 7. Earlier, in the section on Thermodynamic Properties for Ceria, we argued that Reaction 5 is enhanced by the presence of weakly bound oxygen.

Therefore, to promote reaction rates, we looked for dopants for ceria that would facilitate oxygen transfer from ceria.<sup>61–65</sup> The most interesting of these modifiers was praseodymia.<sup>65</sup> Like cerium, praseodymium is a rare-earth metal that readily adopts the +3 and +4 oxidation states; also like ceria, transfer of oxygen was observed from  $\text{Pr}_6\text{O}_{11}$  films to supported Rh particles in high-vacuum studies.<sup>66</sup> The major differences between cerium and praseodymium are that  $\text{PrO}_2$

is produced only with great difficulty and  $\text{Pr}_2\text{O}_3$  forms readily compared to the harsh conditions required to reduce  $\text{CeO}_2$  to  $\text{Ce}_2\text{O}_3$ . As shown by the oxidation isotherms in Figure 9, ceria–praseodymia, solid solutions possess relatively labile oxygen that can be reversibly removed at a  $P(\text{O}_2)$  of  $\sim 10^{-4}$  atm and 973 K. By comparison, the  $P(\text{O}_2)$  need to be below  $\sim 10^{-25}$  atm to significantly reduce  $\text{CeO}_2$  at this temperature. It was, therefore, initially surprising to us that Pd catalysts prepared with ceria–praseodymia supports were much less active than Pd–ceria catalysts for the WGS reaction.<sup>67</sup> Although freshly oxidized catalysts exhibited high activities for short times, the catalysts prepared from ceria–praseodymia-mixed oxides lose their rapidly.

In retrospect, it is easy to understand why the mixed oxides were not active. For Reaction 7 to proceed, the equilibrium  $\text{H}_2:\text{H}_2\text{O}$  ratio must be greater than approximately unity. If this condition is not achieved, it will not be possible to convert a significant fraction of the  $\text{H}_2\text{O}$  to  $\text{H}_2$  through oxidation of the solid. For praseodymia, the stable form of the oxide at a  $\text{H}_2:\text{H}_2\text{O}$  ratio of one is  $\text{Pr}_2\text{O}_3$  for essentially all temperatures. By contrast, equilibrium data for ceria shows that the  $\text{H}_2:\text{H}_2\text{O}$  ratio must be above 100 to have even modest reduction at temperatures below 973 K.<sup>51</sup> It is, therefore, not surprising that we found ceria catalysts to be only slightly reduced under WGS conditions and praseodymia to be completely reduced. Although it was somewhat surprising that the catalytic activities of Pd on ceria–praseodymia-mixed oxides were more similar to Pd/praseodymia than Pd/ceria, calculations suggest that there is a preference for +3 ions to be near the surface of a partially reduced oxide,<sup>68</sup> suggesting that  $\text{Pr}^{+3}$  may migrate to the surface of mixed oxides.

An important implication of these results is that there is an optimal reducibility for the support. The oxygen should not be held so tightly that the oxide cannot be reduced nor so loosely that it cannot react with steam. The equilibrium properties are very useful in this case for providing the target properties of the oxide.

### Conclusions

In this article, I have attempted to demonstrate that fundamental studies into the properties of catalytic materials can provide insights that could lead to new applications. With ceria-supported metals, interactions between the support and the transition metal can lead to catalytic activities that are significantly better than that of the individual components. Understanding these interactions will be the basis for improved catalysts.

### Acknowledgments

This work was supported by the Department of Energy, Office of Basic Energy Sciences, Chemical Sciences, Geosciences and Biosciences Division (Grant DE-FG02-85ER13350). The author thanks his students, who generated most of the ideas in this article. The author acknowledges the helpful ideas from his senior collaborators in this work (Profs John M. Vohs and Paolo Fornasiero, University of Trieste).

### Literature Cited

1. Kung HH, Pellet RJ, Burwell RL. Structure sensitivity in the hydrogenation of hindered hydrocarbons. *J Am Chem Soc.* 1976;98:5603–5611.



2. Tauster SJ, Fung SC, Garten RL. Strong metal-support interactions: group-8 noble metals supported on TiO<sub>2</sub>. *J Am Chem Soc.* 1978; 100:170–175.
3. Demmin RA, Ko CS, Gorte RJ. Effect of titania on the chemisorption and reaction properties of Pt. *J Phys Chem.* 1985;89:1151–1154.
4. Ko CS, Gorte RJ. Characterization of oxide impurities on Pt and their effect on the adsorption of CO and H<sub>2</sub>. *Surf Sci.* 1985;155:296–312.
5. Roberts S, Gorte RJ. A comparison of Pt overlayers on  $\alpha$ -Al<sub>2</sub>O<sub>3</sub>(0001), ZnO(0001), and ZnO(0001). *J Chem Phys.* 1990;98:5337–5344.
6. Roberts SI, Gorte RJ. A study of Pt films on ZrO<sub>2</sub>(100). *J Phys Chem.* 1991;95:5600–5604.
7. Altman EI, Gorte RJ. The desorption of CO from small Pt particles on Al<sub>2</sub>O<sub>3</sub>. *Surf Sci.* 1986;172:71–80.
8. Altman EI, Gorte RJ. A comparison of the desorption of CO from Pt and Rh particles on  $\alpha$ -Al<sub>2</sub>O<sub>3</sub>(0001). *Surf Sci.* 1988;195:392–402.
9. Altman EI, Gorte RJ. The adsorption of NO on small Rh particles on  $\alpha$ -Al<sub>2</sub>O<sub>3</sub>(0001). *J Catal.* 1988;113:185–192.
10. Zafiris GS, Gorte RJ. CO oxidation on Pt/ $\alpha$ -Al<sub>2</sub>O<sub>3</sub>(0001): evidence for structure sensitivity. *J Catal.* 1993;140:418–423.
11. Sugiura M, Ozawa M, Suda A, Suzuki T, Kanazawa T. Development of innovative three-way catalysts containing ceria–zirconia solid solutions with high oxygen storage/release capacity. *Bull Chem Soc Jpn.* 2005;78:752–767.
12. Kaspar J, Fornasiero P, Hickey N. Automotive catalytic converters: current status and some perspectives. *Catal Today.* 2003;77:419–449.
13. Shelef M, Graham GW, McCabe RW. *Ceria and other oxygen storage components in automotive catalysis, Chapter 10.* In: Trovarelli A, editor. *Catalysis by Ceria and Related Materials*. London: Imperial College Press, 2002: 343–375.
14. Ghenciu AF. Review of fuel processing catalysts for hydrogen production in PEM fuel cell systems. *Curr Opin Solid State Mater Sci.* 2002;6:389–399.
15. Liu XS, Ruettinger W, Xu XM, Farrauto R. Deactivation of Pt/CeO<sub>2</sub> water–gas shift catalysts due to shutdown/startup modes for fuel cell applications. *Appl Catal B.* 2005;56:69–75.
16. Bunluesin T, Gorte RJ, Graham GW. Studies of the water–gas-shift reaction on ceria-supported Pt, Pd, and Rh: implications for oxygen-storage properties. *Appl Catal B.* 1998;15:107–114.
17. Hilaire S, Wang X, Luo T, Gorte RJ, Wagner J. A comparative study of water–gas-shift reaction over ceria-supported metallic catalysts. *Appl Catal A.* 2001;215:271–276.
18. Craciun R, Shereck B, Gorte RJ. Kinetic studies of methane steam reforming on ceria-supported Pd. *Catal Lett.* 1998;51:149–153.
19. Farrauto R, Hwang S, Shore L, Ruettinger W, Lampert J, Giroux T, Liu Y, Ilinich O. New material needs for hydrocarbon fuel processing: generating hydrogen for the PEM fuel cell. *Ann Rev Mater Res.* 2003;33:1–27.
20. Heck RM, Farrauto RJ. Automobile exhaust catalysts. *Appl Catal A.* 2001;221:443–457.
21. Möller R, Votsmeier M, Onder C, Guzzella L, Gieshoff J. Is oxygen storage in three-way catalysts an equilibrium controlled process? *Appl Catal.* 2009;91:30–38.
22. Hepburn JS, Dobson A, Gandhi HS. A new test for catalyst oxygen storage which correlates with catalyst performance on the vehicle, SAE paper 942071 (1994).
23. Luo T, Gorte RJ. A mechanistic study of sulfur poisoning of the water–gas-shift reaction over Pd/Ceria. *Catal Lett.* 2003;85:139–146.
24. Eguchi K, Setoguchi T, Inoue T, Arai H. Electrical properties of ceria based oxides and their application to solid oxide fuel cells. *Solid State Ionics.* 1992;300:1–3.
25. Hori CE, Permana H, Ng KYS, Brenner A, More K, Rahmoeller KM, Belton D. Thermal stability of oxygen storage properties in a mixed CeO<sub>2</sub>–ZrO<sub>2</sub> system. *Appl Catal B.* 1998;16:105–117.
26. Zeng Y, Kaytakoglu S, Harrison DP. Reduced cerium oxide as an efficient and durable high temperature desulfurization sorbent. *Chem Eng Sci.* 2000;55:4893–4900.
27. Luo T, Vohs JM, Gorte RJ. An examination of sulfur poisoning on Pd/Ceria catalysts. *J Catal.* 2002;210:397–404.
28. Beck DD, Sommers JW, Dimaggio CL. Impact of sulfur on model palladium-only catalysts under simulated 3-way operation. *Appl Catal B.* 1994;3:205–227.
29. Zafiris GS, Gorte RJ. Evidence for low-temperature migration of oxygen from ceria to Rh. *J Catal.* 1993;139:561–567.
30. Cordatos H, Gorte RJ. CO, NO, and H<sub>2</sub> adsorption on ceria-supported Pd. *J Catal.* 1996;159:112–118.
31. Demmin RA, Gorte RJ. Design parameters for temperature-programmed desorption from a packed bed. *J Catal.* 1984;90:32–39.
32. Gorte RJ. Design parameters for temperature programmed desorption from porous catalysts. *J Catal.* 1982;75:164–174.
33. Cordatos H, Bunluesin T, Gorte RJ. Study of CO, NO, and H<sub>2</sub> adsorption on model Pd/ $\alpha$ -Al<sub>2</sub>O<sub>3</sub>(0001). *Catal Surf Sci.* 1995;323: 219–227.
34. Smirnov MY, Graham GW. Pd oxidation under UHV in a model Pd/ceria-zirconia catalyst. *Catal Lett.* 2001;72:39–44.
35. Zafiris GS, Gorte RJ. Evidence for a second CO oxidation mechanism on Rh/Ceria. *J Catal.* 1993;143:86–91.
36. Bunluesin T, Cordatos H, Gorte RJ. A study of CO oxidation kinetics on Rh/ceria. *J Catal.* 1995;157:222–226.
37. Oh SH, Eickel CC. Effects of cerium addition on CO oxidation kinetics over alumina supported rhodium catalysts. *J Catal.* 1988; 134:543–555.
38. Bunluesin T, Putna ES, Gorte RJ. A comparison of CO oxidation on ceria-supported Pt, Pd, and Rh. *Catal Lett.* 1996;41:1–5.
39. Luo T, Gorte RJ. A mechanistic study of sulfur poisoning of the water–gas-shift reaction over Pd/ceria. *Catal Lett.* 2003;85:139–146.
40. Sharma S, Hilaire S, Vohs JM, Gorte RJ, Jen HW. Evidence for oxidation of ceria by CO<sub>2</sub>. *J Catal.* 2000;190:199–204.
41. Wang X, Gorte RJ. A study of steam reforming of hydrocarbon fuels on Pd/ceria. *Appl Catal A.* 2002;224:209–218.
42. Wang X, Gorte RJ. Steam reforming of n-butane on Pd/ceria. *Catal Lett.* 2001;73:15–19.
43. Di Monte R, Kaspar J. On the role of oxygen storage in three-way catalysis. *Top Catal.* 2004;28:47–57.
44. Park S, Craciun R, Vohs JM, Gorte RJ. Direct oxidation of hydrocarbons in a solid oxide fuel cell I. Methane oxidation. *J Electrochem Soc.* 1999;146:3603–3605.
45. Beck DD, Sommers JW, Dimaggio CL. Axial characterization of oxygen storage capacity in close-coupled lightoff and underfloor catalytic converters and impact of sulfur. *Appl Catal B.* 1997;11:273–290.
46. Cordatos H, Bunluesin T, Stubenrauch J, Vohs JM, Gorte RJ. Effect of ceria structure on oxygen migration for Rh/ceria catalysts. *J Phys Chem.* 1996;100:785–789.
47. Putna ES, Gorte RJ, Vohs JM, Graham GW. Evidence for enhanced dissociation of CO on Rh/ceria. *J Catal.* 1998;178:598–603.
48. Bunluesin T, Gorte RJ, Graham GW. CO oxidation for the characterization of reducibility in oxygen storage components of three-way automotive catalysts. *Appl Catal B.* 1997;14:105–115.
49. Bunluesin T, Gorte RJ, Graham GW. Studies of the water–gas-shift reaction on ceria-supported Pt, Pd, and Rh: implications for oxygen-storage properties. *Appl Catal B.* 1998;15:107–114.
50. Mogensen M, Sammes NM, Tompsett GA. Physical, chemical and electrochemical properties of pure and doped ceria. *Solid State Ionics.* 2000;129:63–94.
51. Zhou G, Shah PR, Montini T, Fornasiero P, Gorte RJ. Oxidation enthalpies for reduction of ceria surfaces. *Surf Sci.* 2007;601:2512–2519.
52. Shah PR, Kim T, Zhou G, Fornasiero P, Gorte RJ. Evidence for entropy effects in the reduction of ceria-zirconia solutions. *Chem Mater.* 2006;18:5363–5369.
53. Kim T, Vohs JM, Gorte RJ. A thermodynamic investigation of the redox properties of ceria-zirconia solid solutions. *Ind Eng Chem.* 2006;45:5561–5565.
54. Zhou G, Shah PR, Kim T, Fornasiero P, Gorte RJ. Oxidation entropies and enthalpies for ceria-zirconia mixed oxides. *Catal Today.* 2007;123:86–93.
55. Mamontov E, Egami T. Structural defects in a nano-scale powder of CeO<sub>2</sub> studied by pulsed neutron diffraction. *J Phys Chem Solids.* 2000;61:1345–1356.
56. Da Silva JLF, Ganduglia-Pirovano MV, Sauer J. Formation of the cerium orthovanadate CeVO<sub>4</sub>: DFT+U study. *Phys Rev B.* 2007;76: 125117.
57. Reidy RF, Swider KE. Determination of the cerium oxidation state in cerium vanadate. *J Am Ceram Soc.* 1995;78:1121–1122.
58. Shah PR, Khader MM, Vohs JM, Gorte RJ. A comparison of the redox properties of vanadia-based mixed oxides. *J Phys Chem C.* 2008;112:2613–2617.

59. Putna ES, Vohs JM, Gorte RJ. Oxygen desorption from  $\alpha$ -Al<sub>2</sub>O<sub>3</sub>(0001) supported Rh, Pt and Pd particles. *Surf Sci.* 1997;391: L1178–L1182.
60. Ferrizz RM, Gorte RJ, Vohs JM. TPD and XPS investigation of the interaction of SO<sub>2</sub> and ceria. *Catal Lett.* 2002;82:123–129.
61. Gorte RJ, Zhao S. Studies of the water–gas-shift reaction with ceria-supported precious metals. *Catal Today.* 2005;104:18–24.
62. Zhao S, Luo T, Gorte RJ. Deactivation of the water–gas-shift activity of Pd/ceria by Mo. *J Catal.* 2004;221:413–420.
63. Zhao S, Gorte RJ. A comparison of ceria and Sm-doped ceria for hydrocarbon oxidation reactions. *Appl Catal A.* 2004;277:129–136.
64. Zhou G, Hanson J, Gorte RJ. A thermodynamic investigation of the redox properties of ceria-titania mixed oxides. *Appl Catal A.* 2008;335:153–158.
65. Zhou G, Gorte RJ. Thermodynamic investigation of the redox properties for ceria-hafnia, ceria-terbia, and ceria-praseodymia solid solutions. *J Phys Chem B.* 2008;112:9869–9875.
66. Putna ES, Vohs JM, Gorte RJ, Graham GW. An examination of praseodymia as an oxygen-storage component in three-way catalysts. *Catal Lett.* 1998;54:17–21.
67. Bakhmutsky K, Zhou G, Timothy S, Gorte RJ. The water–gas-shift reaction on pd/ceria-praseodymia: the effect of redox thermodynamics. *Catal Lett.* 2009;129:61–65.
68. Cordatos H, Ford D, Gorte RJ. Simulated annealing study of the structure and reducibility in ceria clusters. *J Phys Chem.* 1996;100: 18128–18132.

*Manuscript received Aug. 6, 2009, revision received Dec. 23, 2009, and final revision received Feb. 23, 2010.*